analytical chemistry

Article

pubs.acs.org/ac

Ultrasensitive Electrochemical Detection of Prostate-Specific Antigen by Using Antibodies Anchored on a DNA Nanostructural Scaffold

Xiaoqing Chen,[†,∥] Guobao Zhou,[†,‡,∥] Ping Song,[‡] Jingjing Wang,[‡,§] Jimin Gao,[§] Jianxin Lu,[§] Chunhai Fan,[‡] and Xiaolei Zuo*[,‡]

[†]School of Chemistry and Chemical Engineering, Collaborative Innovation Center of Resource-conserving & Environment-friendly Society and Ecological Civilization, Central South University, Changsha, Hunan 410083, China

[‡]Division of Physical Biology and Bioimaging Center, Shanghai Synchrotron Radiation Facility, Shanghai Institute of Applied Physics, Chinese Academy of Sciences, Shanghai, 201800, China

[§]School of Medical Lab Science and Life Science, Wenzhou Medical University, Wenzhou, Zhejiang 325035, China

Supporting Information

ABSTRACT: The high occurrence of prostate cancer in men makes the prostate-specific antigen (PSA) screening test really important. More importantly, the recurrence rate after radical prostatectomy is high, whereas the traditional PSA immunoassay does not possess the sufficient high sensitivity for post-treatment PSA detection. In these assays, uncontrolled and random orientation of capture antibodies on the surface largely reduces their activity. Here, by exploiting the rapidly emerging DNA nanotechnology, we developed a DNA nanostructure based scaffold to precisely control the assembly of antibody monolayer. We demonstrated that the detection sensitivity was critically dependent on the nanoscale-spacing (nanospacing) of immobilized antibodies. In addition to the controlled assembly, we further amplified the sensing signal by using the gold nanoparticles, resulting in extremely high sensitivity and a low detection limit of 1 pg/mL. To test the real-world applicability of our nanoengineered electrochemical sensor, we evaluated the performance with 11 patients' serum samples and obtained consistent results with the "gold-standard" assays.

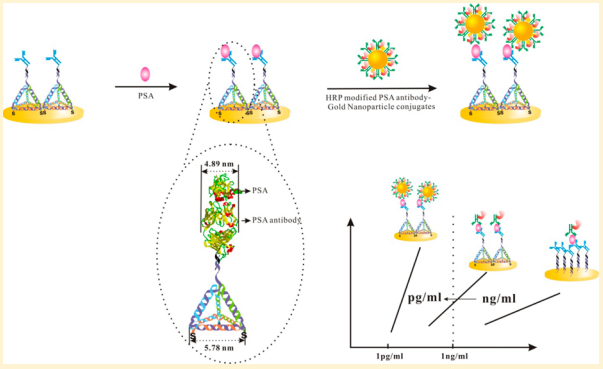

Prostate cancer is the most common cancer in American men. One man out of six will be diagnosed with prostate cancer; moreover, the occurrence rate increases greatly in older men (aged 65 or older).[1] Thus, the sensitive detection of serum biomarkers of prostate cancer is really important and urgent for the early detection of prostate cancer.[2−7] Prostate specific antigen (PSA) secreted by prostatic epithelial cells is a classic biomarker for screening of prostate cancer. Due to the high recurrence rate of prostate cancer after treatment, PSA is also an efficient indicator to predict the recurrence certainly.[2−8]

However, for commercially available immunoassays of PSA, good precision can be achieved at relatively higher PSA levels, but intralaboratory coefficients of variation at lower PSA levels are quite large which may cause difficulty in determining the early detection of prostate cancer and cancer recurrence after treatment.[9] The underlying physicochemical principle is that, in traditional immunoassays, capture antibodies are physically adsorbed or covalently immobilized on a solid surface in a random pattern,[10,11] and after the antigen binding, signal antibodies are used to produce a detectable signal. Due to the lack of nanotechnology to control the orientation and density of antibodies, the binding affinity of antibodies on the surface are largely limited by the unordered immobilization.[11−16] Many antibodies may lose their binding activities completely if the active sites are embedded in the antibody layer or forced to the solid surface. This may eventually affect the sensitivity and reproducibility of the assays.

DNA nanotechnology is emerging as a novel nanotechnology with several unique advantages including a highly programmable nature, high precision, and ease of preparation. On the basis of these, various DNA nanostructures are designed from 1-dimension (1D) to 2-dimension (2D) and 3-dimension (3D).[17−24] Because the basic block is a DNA base pair, which is only 0.34 nm for one base pair, the DNA nanostructure can be precisely controlled in size. The programmable folding nature of DNA can be used to design arbitrary shapes of DNA nanostructures. We also noticed that the DNA structures have comparable dimensions to the molecular recognition units (such as DNA probes, antibodies, and aptamers). DNA nanostructures would be ideal scaffolds for the control of these recognition units, through which we can investigate the

Received: January 6, 2014
Accepted: June 26, 2014
Published: June 26, 2014

   dx.doi.org/10.1021/ac500054x | *Anal. Chem.* 2014, 86, 7337−7342

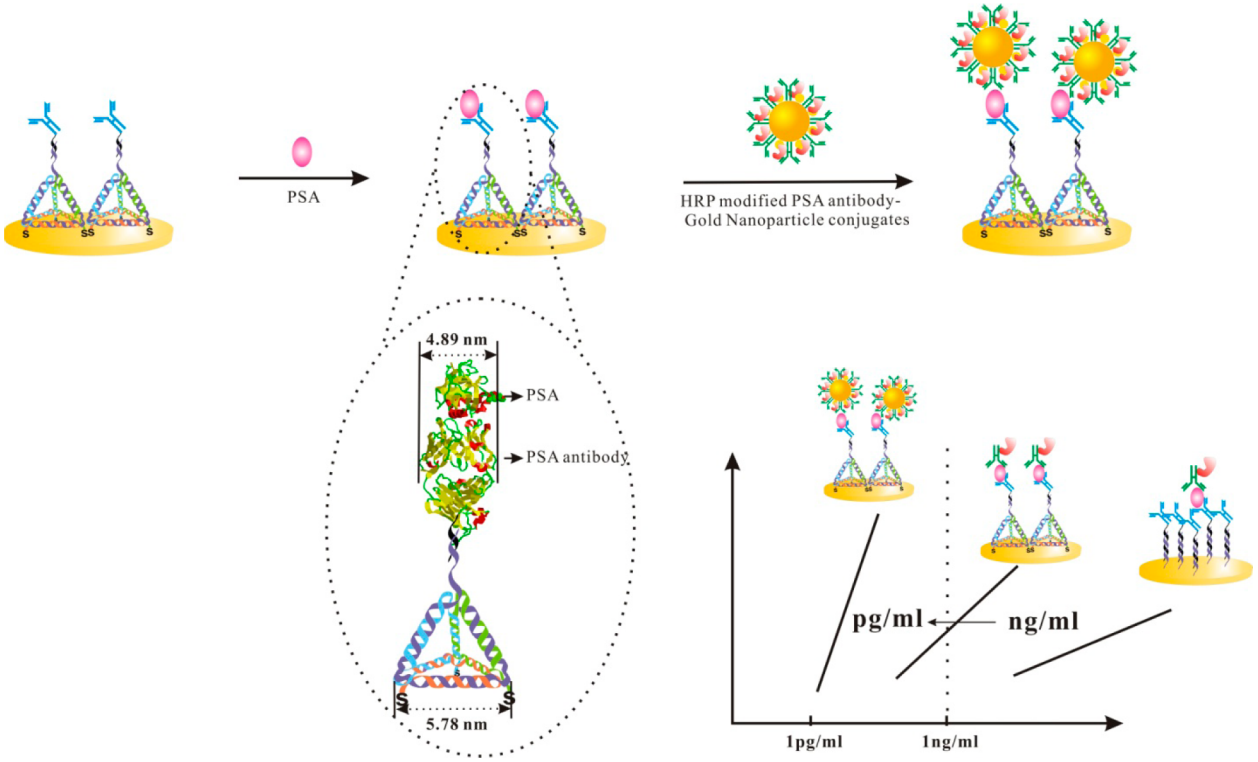

Figure 1. We use the DNA nanostructure (here, a tetrahedron, each edge of the tetrahedron contains 17 base pairs, which is ~5.78 nm and comparable to the size of the PSA antibody (~4.89 nm)) as the scaffold to increase the nanospacing, which can effectively improve the binding efficiency and detection sensitivity. We combine the DNA tetrahedron based surface control and the HRP-antibody-gold nanoparticle conjugates to amplify the signal. The detection limit is as low as 1 pg/mL. The nanospacing of antibodies is relatively small by using double stranded DNA (ds-DNA, that contains the same linker with that on the tetrahedron and a supporting single stranded DNA of 10 bases) as the scaffold for the immobilization of antibodies. Thus, the binding efficiency of antibodies is low because many active sites are blocked. The measurement of the 3-dimensional structure of PSA antibody was obtained from the PDB (protein data bank) Web site (http://www.rcsb.org/pdb/home/home.do).

Table 1. DNA Sequences Used in Our Experiments

	DNA sequence (5′−3′)
A	ACATTCCTAAGTCTGAAACATTACAGCTTGCTACACGAGAAGAGCCGCCATAGTATTTTTTTTTTGTATCCAGTGGCTCA
B	HS-TATCACCAGGCAGTTGACAGTGTAGCAAGCTGTAATAGATGCGAGGGTCCAATAC
C	HS-TCAACTGCCTGGTGATAAAACGACACTACGTGGGAATCTACTATGGCGGCTCTTC
D	HS-TTCAGACTTAGGAATGTGCTTCCCACGTAGTGTCGTTTGTATTGGACCCTCGCAT
linker	HC≡C-TGAGCCACTGGATAC
E	HS-TTTTTTTTTTGTATCCAGTGGCTCA

effects of nanospacing between recognition molecules in such a precise way. For example, the tetrahedron has been employed as a scaffold for the detection of DNA and microRNA, which provided a superior environment for the biorecognition process. The advantages include the well controlled density and orientation of DNA bioprobes and minimized nonspecific adsorption on the surface.[18−21,23,24]

Although the orientation of antibody immobilization has been investigated via the conserved nucleotide binding site, the native thiol-groups directly coupled to the gold, and defined chemical linkages at the solid−liquid interface,[11−13,15] spatial control of antibody immobilization remains to be a key challenge in immunological detection. The nanoscale-resolution offered by DNA nanostructures provides an unprecedented ability to precisely control the antibody anchoring. By using the DNA nanostructural probes, we did provide a solution to the key problem in immunological detection. As an excellent demonstration of the effect, the detection limit of PSA was lowered from a high level of picograms to 1 picogram in this work. We controlled the surface immobilization of antibodies with the DNA tetrahedron. Systematically, we investigated the effects of nanospacing between antibodies on the detection sensitivity by comparing the DNA tetrahedron based antibody immobilization and double stranded DNA (ds-DNA) based antibody immobilization (Figure 1). Interestingly, we found that the detection sensitivity was critically dependent on the nanospacing of immobilized antibodies. Then, we used the enzyme modified gold nanoparticles[25] as signal amplifier based on the DNA tetrahedron scaffold, and we obtained a detection limit of 1 pg/mL PSA, which is sensitive enough to monitor the prognosis of prostate cancer.

■ EXPERIMENTAL SECTION

Reagents and Materials. Cu powder was purchased from Sinopharm Chemical Reagent Co. Ltd. 3-(Azidotetra-(ethyleneoxy)) propionic acid succinimidyl ester (AEPS) and the DNA sequences shown in Table 1 were synthesized and purified by Invitrogen. Gold nanoparticles (20 nm in diameter)

dx.doi.org/10.1021/ac500054x | Anal. Chem. 2014, 86, 7337−7342

with a concentration of 1.16 nM were purchased from Ted Pella, Inc. Dimethyl sulfoxide (DMSO), acetonitrile, 6-mercapto-1-hexanol (MCH), horseradish peroxidase (HRP), casein, bovine serum albumin (BSA), Tween 20 (T20), Bis (*p*-sulfonatophenyl) phenylphosphine dehydrate dipotassium salt (BSPP), Tris (2-carboxyethyl) phosphine hydrochioride (TCEP), Tris-[(1-benzyl-1*H*-1,2,3-triazol-4-yl)methyl] amine (TBTA), and 3,3′-dithiodipropionic acid di(*N*-hydroxysuccinimide ester) (DTSP) were purchased from Sigma-Aldrich.

Prostate-specific antigen (PSA, from human seminal fluid) and PSA monoclonal antibody (Ab1) were purchased from US Biological and Fitzgerald, respectively. PSA antibody modified with horseradish peroxidase (Ab2-HRP) was from Shanghai Linc-Bioscience Co. Ltd. Ab1, PSA, and Ab2-HRP were dissolved in PBS (10 mM in phosphate, 0.14 M NaCl, 2.7 mM KCl, pH 7.4), containing 1% BSA and 1% BSA + 1% casein, respectively. TMB substrate (TMB = 3,3′,5,5′tetramethylbenzidine, enhanced K-blue activity substrate, H_2O_2 included) was purchased from Neogen. The chemicals mentioned were used without further purification, and Milli-Q water (18 MΩ·cm resistivity) was used throughout all experiments.

Instrument. An electrochemical workstation (model CHI 1130b) was used for cyclic voltammetry and amperometry detection in a conventional three-electrode cell, including a platinum counter electrode, a reference electrode (Ag/AgCl, 3 M KCl), and a gold working electrode. Cyclic voltammetry was performed from 0 to 0.7 V at a scan rate of 100 mV/s. Amperometric detection was carried out at 100 mV, and the steady state of HRP redox reaction could usually be obtained within 100 s. The electrochemiluminescence immunoassays for the PSA detection of patients' samples were carried out by using a ROCHE Elecsys 2010 Analyzer (with a service kit, REF: 04641655 190).

Self-Assembly of DNA Probes on Gold Electrode Surfaces. Gold electrodes (2 mm diameter) were cleaned according to the reported protocol.[26,27] Tetrahedral nanostructure based probes (TSP) were prepared, and the surface density of TSP on the electrode was measured as outlined in the reported technique.[28,29] The five strands (A, B, C, D, and Linker) were mixed in TM buffer (20 mM Tris, 50 mM $MgCl_2$, pH 8.0) with a final concentration of 1 μM, then heated to 95 °C for 2 min, and cooled to 4 °C within 30 s by using PTC-200 (MJ. Research Inc., SA). The formation of the tetrahedron in solution was confirmed through polyacrylamide gel electrophoresis (PAGE, Figure S1, Supporting Information). We also characterized the tetrahedron on the mica surface (Figure S2, Supporting Information). We found that it was relatively uniformly distributed on the surface. Next, gold electrodes were incubated with 3 μL of TSP (1 μM) overnight at room temperature. The thiolated double-stranded probe (dsP) was immobilized on the gold electrode using the same process; 3 μL of 1 μM double strand in TM buffer was dropped to the surface of the gold electrode and incubated overnight at room temperature. The resulting TSP and dsP electrodes were rinsed with PBS.

Modification of Gold Nanoparticles (AuNPs). First, AuNPs were protected by BSPP. Next, 5 mL of Au/BSPP NPs (~1.2 nM) mixed with DTSP (500 μL, 5 mM, in acetonitrile) was gently shaken for 3 h at 25 °C. The abundant DTSP was washed away with 1 mL of PBS/T three times. Thereafter, the precipitation suspended in PB (250 μL, 10 mM, pH 7.4) was mixed with 250 μL of Ab2-HRP. After incubation for 1 h, 500 μL of 5% BSA solution was injected to passivate the reaction mixture for 30 min. Finally, nanoconjugates were suspended in 250 μL of 1% BSA + 1% casein after being washed with PBS/T three times and stored at 4 °C for further use.

dsP and TSP Based Sandwich Assays. Each TSP or dsP modified electrode was incubated with 100 μL of click reaction solution, which contains 10 mM $CuSO_4$ (10 μL), 10 mM TBTA (10 μL), 10 mM TCEP (10 μL), 0.1 M PB (10 μL, pH 7.4), DMSO (40 μL), Q-H_2O (19.5 μL), 5 mM AEPS (0.5 μL), and a proper amount of Cu powder. After reacting in the dark at room temperature for 3 h, electrodes were rinsed with PBS/T to remove unfixed AEPS. Then, Ab1 was covalently linked to AEPS on the surface of the electrode by treatment with 3 μL of the reaction mixture (20 μL of 0.2 mg/mL Ab1, 2 μL of 1 M $NaHCO_3$) for 1 h. Unbounded Ab1 was washed away with PBS/T; then, the electrodes were incubated with 2 μL of PBS solution (with 1% BSA) containing various concentrations of PSA for 1 h. At last, the electrodes were incubated with 2 μL of Ab2-HRP (10 μg/mL) or 20 nM nanoconjugates for 1 h and rinsed thoroughly with PBS/T; sensors were then ready for the electrochemical measurements in 3 mL of TMB solution. The calculation of the amount of HRP on the surface was based on the well established method.[30]

RESULTS AND DISCUSSION

The immobilization of antibodies through physical adsorption is not used in our study since it is difficult to control the orientation, density, and monodispersity of antibodies at the surface. Here, we first immobilized double stranded DNA on the gold surface through the well established gold−thiol bond. To realize the well oriented antibody immobilization, we employed a densely packed monolayer to ensure the upright orientation of double stranded DNA. Alkyne groups were modified on the far end of the double stranded DNA, which can participate in the subsequent click reaction. Then, the capture antibodies can be conjugated on the double stranded DNA (Figure 1) via the high efficient click chemistry. By using this method, we can obtain a well-controlled antibody monolayer on the surface. A sandwich type assay was employed in our investigation. After the capture of the antigen-PSA, HRP (horseradish peroxidase) modified signaling antibody was employed to produce an enzymatic catalytic signal in the solution with substrates, which can be readily detected by using the electrochemical method. Then, we investigated the analytical capability of this sensor for PSA detection and obtained a detection limit of 10 ng/mL. This detection limit is relatively poor and can only be used to detect a high level of PSA. By using this system, we determined that the density of the double stranded DNAs is $1.7 \times 10^{13}/cm^2$ (Figure 2), and we can estimate that the distance between the double stranded DNAs is ~2.4 nm (Figure S3, Supporting Information). As a result, the capture antibodies that were conjugated in this pattern were crowded and inhibited the binding activity of the antibodies. The effective binding sites could be reduced by an order of magnitude or more when many of the active sites were blocked.[10] Enlarging the nanospacing would be a benefit to the antigen binding.

To verify our hypothesis and to improve the sensitivity, we increased the nanospacing between the capture antibodies by using the relatively rigid DNA tetrahedron. Using the same conjugation steps, we attached the capture antibodies on the pattern of the DNA tetrahedra. The nanospacing between the DNA linkers is ~5.0 nm (Figure S3, Supporting Information),

dx.doi.org/10.1021/ac500054x | *Anal. Chem.* 2014, 86, 7337−7342

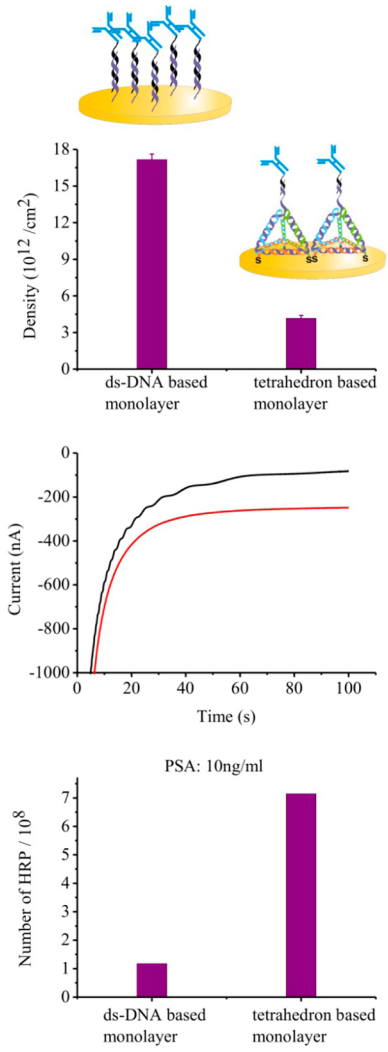

Figure 2. (top) The surface densities of ds-DNA and the tetrahedron on the gold surface were detected by the quantitative adsorption of $[Ru(NH_3)_6]^{3+}$. The density of ds-DNA is higher than the density of the tetrahedron. (middle) *i*–*t* curves from the tetrahedron based sandwich assay (red) and the ds-DNA based sandwich assay (black), respectively. (bottom) The HRPs that attached on the gold surface through the sandwich assay were calculated via the electrocatalytic current. At 10 ng/mL PSA, the amount of HRP captured on the tetrahedron based monolayer is 6 times higher than that on the ds-DNA based monolayer.

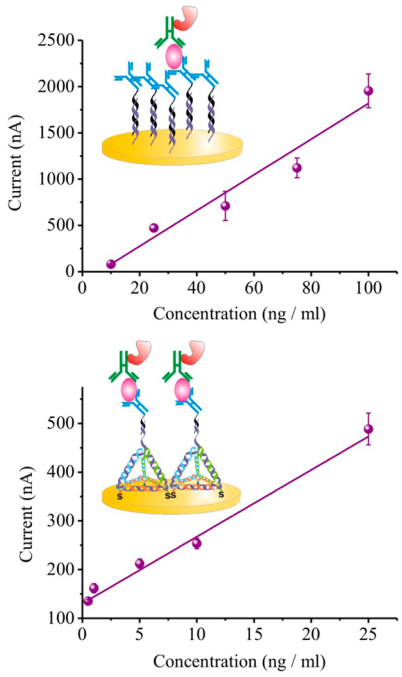

Figure 3. Titration curves obtained from the ds-DNA based monolayer (top) and the tetrahedron based monolayer (bottom) with a sandwich detection strategy. HRP modified signaling antibodies were used to produce the electrocatalytic signal. The detection limits were 10 ng/mL and 500 pg/mL, respectively.

which is comparable to the dimensions of capture antibody (Figure 1). At this condition, the binding activity of capture antibodies should be retained well by minimizing the steric effect and the entanglement between antibodies. As a result, we obtained a higher electrochemical current (Figure 2, middle) which indicated more enzyme modified signaling antibodies were bound. We calculated the amount of horseradish peroxidase (HRP) that attached on the surface when the PSA concentration was 10 ng/mL. By using this, we can estimate the binding efficiency of the immobilized monolayer. Impressively, the amount of HRP attached on the tetrahedron based surface is ~6 times more than that on the ds-DNA based surface (Figure 2, bottom). Then, we used this system to detect PSA and obtained a detection limit of 500 pg/mL (Figure 3). The sensitivity was improved ~20 times. These results above indicate that the control of the nanospacing between the capture antibodies leads to a better binding activity and improved detection sensitivity.

The sensitivity of 500 pg/mL is acceptable for routine screening of prostate cancer but not high enough to monitor the recurrence of prostate cancer after treatment. To further improve the sensitivity, we attempted to employ the gold nanoparticles[25] as the signal amplifier to amplify the detection. Through the amplification, one binding event would bring more HRP enzymes to produce catalytic signal (Figure S4, Supporting Information). Interestingly, we found that the nanospacing between the antibodies also affect the amplification system. At the nanospacing of 2.4 nm, we amplified the detection. The detection limit was 50 pg/mL (Figure 4). At the nanospacing of 5.0 nm, impressively, we obtained the detection limit of 1 pg/mL (Figure 4). With further enlarged nanospacing, we could further improve the sensor signal by using a dilution strategy. That is, we used tetrahedra without probes, on which antibodies cannot be attached. The results indicated that the optimal ratio was ~1:50 (Figure S5, Supporting Information). On the basis of the previous study, for the patients who have a postoperative and persistent PSA level below 5 pg/mL, there is no evidence of recurrence.[6] Our sensitivity is high enough to monitor the recurrence of prostate cancer.

Moreover, the specificity of our method is excellent. A high concentration of CEA (carcinoembryonic antigen, 10 μg/mL) or AFP (α-fetoprotein, 10 μg/mL) can only produce signals like the background (Figure 5), while a signal from a much lower concentration of PSA (25 ng/mL) is much higher than that from CEA and AFP (Figure 5).

Next, to test and verify the practical application of our method, we collected 11 patients' serum samples from the local hospital and then detected the PSA levels of them. We can differentiate the PSA levels clearly between the patients' serum

dx.doi.org/10.1021/ac500054x | *Anal. Chem.* 2014, 86, 7337–7342

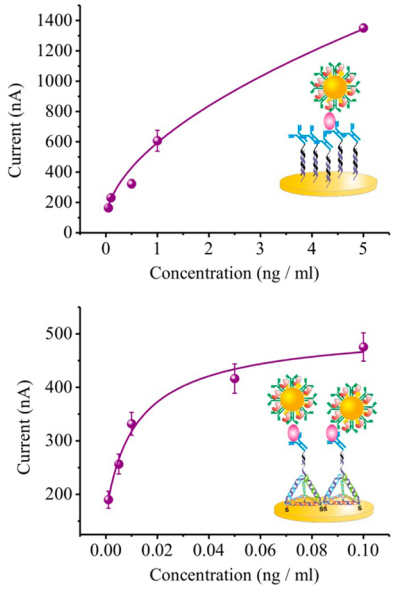

Figure 4. Titration curves obtained from the ds-DNA based monolayer (top) and the tetrahedron based monolayer (bottom) with gold nanoparticle amplification. The detection limits were 50 and 1 pg/mL, respectively.

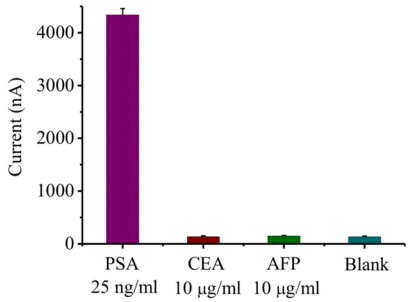

Figure 5. Detection specificity was challenged with a high concentration (10 μg/mL) of CEA and AFP which only produced a relatively small signal. Twenty-five ng/mL of PSA can produce a much higher signal.

and normal serum (Figure 6). Then, after we analyzed the PSA levels of all 11 samples, we compared our results to those obtained from the local hospital (with the "gold-standard" chemiluminescence). Our results agree well with the results from the hospital which indicates the potential clinical applications of our method. As in our previous study, the DNA tetrahedron modified biosensing surface has a high resistance to the nonspecific adsorption[20] and this advantage ensures our present study performs well in complicated real samples.

Finally, our method can be generalized to the biomarkers related to some other biomarkers. When we used the capture antibodies for CEA and AFP, these two biomarkers can be easily detected, respectively. The signal to background ratio is high by using our strategy (Figure 7).

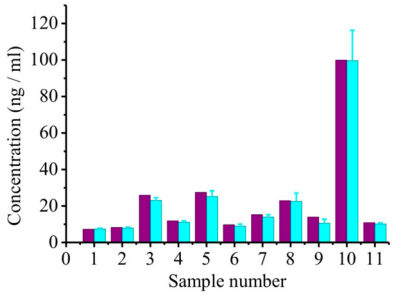

Figure 6. Eleven serum samples of patients were collected from the local hospital and detected by using our method. Then, the results were compared to those obtained from the local hospital. Our results were highly consistent with the results from hospital.

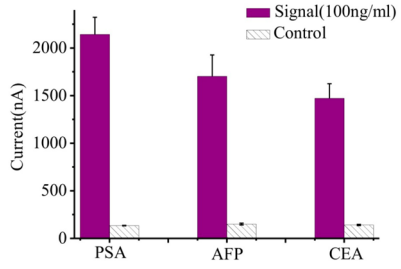

Figure 7. To generalize our strategy to the detection of other biomarkers, we changed the capture antibodies to those responsive to AFP and CEA. We obtained an obvious signal increase over the background.

CONCLUSION

In summary, we used the double stranded DNA and the DNA tetrahedron as the scaffold to control the density of antibodies. Compared to some other technologies, DNA nanotechnology has several advantages. First, DNA nanostructures are easy to prepare just though the simple heat-annealing process. Second, the DNA nanostructures have highly uniform dimensions. Third, it is easy to conjugate biomolecules to DNA nanostructures. By using the DNA nanotechnology, we can interrogate the nanospacing effects of capture probes in such a precise way. At last, we achieved sensitive and specific PSA detection which is useful both in screening of prostate cancer and in monitoring the recurrence of prostate cancer. The patients' samples tested well, and the results were highly consistent with those from the hospital. Our strategy can be generalized to many other biomarkers as well.

ASSOCIATED CONTENT

Supporting Information

Additional information as noted in text. This material is available free of charge via the Internet at http://pubs.acs.org.

AUTHOR INFORMATION

Corresponding Author

*E-mail: zuoxiaolei@sinap.ac.cn. Tel: (86) 21 39194727. Fax: (86) 21 39194173.

Author Contributions

‖Xiaoqing Chen and Guobao Zhou contributed equally.

Notes

The authors declare no competing financial interest.

ACKNOWLEDGMENTS

This work was supported by National Natural Science Foundation of China (Grant No. 21175155), Hunan Provincial Innovation Foundation for Postgraduate, the National Basic

Research Program of China (973 Program 2012CB932600), 100-talent project from Chinese Academy of Sciences, and Shanghai Pujiang Project with Grant No. 13PJ1410700.

REFERENCES

(1) National Cancer Institute, http://www.cancer.gov/cancertopics/types/prostate, accessed Jan 3, 2014.
(2) Lance, R. S.; Drake, R. R.; Troyer, D. A. *Expert Rev. Anticancer Ther.* **2011**, *11*, 1341−1343.
(3) Mohan, K.; Donavan, K. C.; Arter, J. A.; Penner, R. M.; Weiss, G. A. *J. Am. Chem. Soc.* **2013**, *135*, 7761−7767.
(4) Nam, J. M.; Thaxton, C. S.; Mirkin, C. A. *Science* **2003**, *301*, 1884−1886.
(5) Tavoosidana, G.; Ronquist, G.; Darmanis, S.; Yan, J. H.; Carlsson, L.; Wu, D.; Conze, T.; Ek, P.; Semjonow, A.; Eltze, E.; Larsson, A.; Landegren, U. D.; Kamali-Moghaddam, M. P. *Natl. Acad. Sci. U.S.A.* **2011**, *108*, 8809−8814.
(6) Thaxton, C. S.; Elghanian, R.; Thomas, A. D.; Stoeva, S. I.; Lee, J. S.; Smith, N. D.; Schaeffer, A. J.; Klocker, H.; Horninger, W.; Bartsch, G.; Mirkin, C. A. P. *Natl. Acad. Sci. U.S.A.* **2009**, *106*, 18437−18442.
(7) Walsh, P. C. J. *Urology* **2010**, *183*, 1838−1838.
(8) Gao, Z. Q.; Xu, M. D.; Hou, L.; Chen, G. N.; Tang, D. P. *Anal. Chem.* **2013**, *85*, 6945−6952.
(9) Bock, J. L.; Klee, G. G. *Arch. Pathol. Lab. Med.* **2004**, *128*, 341−343.
(10) Squires, T. M.; Messinger, R. J.; Manalis, S. R. *Nat. Biotechnol.* **2008**, *26*, 417−426.
(11) Yoshimoto, K.; Nishio, M.; Sugasawa, H.; Nagasaki, Y. *J. Am. Chem. Soc.* **2010**, *132*, 7982−7989.
(12) Alves, N. J.; Kiziltepe, T.; Bilgicer, B. *Langmuir* **2012**, *28*, 9640−9648.
(13) Kausaite-Minkstimiene, A.; Ramanaviciene, A.; Kirlyte, J.; Ramanavicius, A. *Anal. Chem.* **2010**, *82*, 6401−6408.
(14) Laing, S.; Irvine, E. J.; Hernandez-Santana, A.; Smith, W. E.; Faulds, K.; Graham, D. *Anal. Chem.* **2013**, *85*, 5617−5621.
(15) Liu, Y. W.; Ogorzalek, T. L.; Yang, P.; Schroeder, M. M.; Marsh, E. N. G.; Chen, Z. *J. Am. Chem. Soc.* **2013**, *135*, 12660−12669.
(16) Seo, J. S.; Lee, S.; Poulter, C. D. *J. Am. Chem. Soc.* **2013**, *135*, 8973−8980.
(17) Goodman, R. P.; Schaap, I. A. T.; Tardin, C. F.; Erben, C. M.; Berry, R. M.; Schmidt, C. F.; Turberfield, A. J. *Science* **2005**, *310*, 1661−1665.
(18) Lu, N.; Pei, H.; Ge, Z. L.; Simmons, C. R.; Yan, H.; Fan, C. H. *J. Am. Chem. Soc.* **2012**, *134*, 13148−13151.
(19) Pei, H.; Liang, L.; Yao, G. B.; Li, J.; Huang, Q.; Fan, C. H. *Angew. Chem., Int. Ed.* **2012**, *51*, 9020−9024.
(20) Pei, H.; Lu, N.; Wen, Y. L.; Song, S. P.; Liu, Y.; Yan, H.; Fan, C. H. *Adv. Mater.* **2010**, *22*, 4754−4758.
(21) Pei, H.; Zuo, X. L.; Pan, D.; Shi, J. Y.; Huang, Q.; Fan, C. H. *NPG Asia Mater.* **2013**, *5*, No. e51.
(22) Shen, W. Q.; Zhong, H.; Neff, D.; Norton, M. L. *J. Am. Chem. Soc.* **2009**, *131*, 6660−6661.
(23) Wen, Y. L.; Pei, H.; Shen, Y.; Xi, J. J.; Lin, M. H.; Lu, N.; Shen, X. Z.; Li, J.; Fan, C. H. *Sci. Rep.-UK* **2012**, *2*, 867.
(24) Wen, Y. L.; Pei, H.; Wan, Y.; Su, Y.; Huang, Q.; Song, S. P.; Fan, C. H. *Anal. Chem.* **2011**, *83*, 7418−7423.
(25) Lin, M. H.; Pei, H.; Yang, F.; Fan, C. H.; Zuo, X. L. *Adv. Mater.* **2013**, *25*, 3490−3496.
(26) Xiao, Y.; Lai, R. Y.; Plaxco, K. W. *Nat. Protoc.* **2007**, *2*, 2875−2880.
(27) Zhang, J.; Song, S. P.; Wang, L. H.; Pan, D.; Fan, C. H. *Nat. Protoc.* **2007**, *2*, 2888−2895.
(28) Abi, A.; Ferapontova, E. E. *J. Am. Chem. Soc.* **2012**, *134*, 14499−14507.
(29) Lao, R. J.; Song, S. P.; Wu, H. P.; Wang, L. H.; Zhang, Z. Z.; He, L.; Fan, C. H. *Anal. Chem.* **2005**, *77*, 6475−6480.
(30) Liu, G. Z.; Paddon-Row, M. N.; Gooding, J. J. *Electrochem. Commun.* **2007**, *9*, 2218−2223.